Int. J. Electrochem. Sci., 16 **(2021)** Article ID: 210950, doi: 10.20964/2021.08.44

International Journal of
ELECTROCHEMICAL
SCIENCE
www.electrochemsci.org

Modification of a Carbon Paste Electrode with a ZnO@ZIF-8 Nanocomposite and Fabrication of a Highly Sensitive Electrochemical Sensor for Sulfamethoxazole Detection

Shaofei Guo[*], *Xiaoyu Chen, Yuetao Ling, Han Wang, Xin Wei, Ruihua Pan and Peng Wang*

15 Jinyinhu Road, Dongxihu District, Technology Center of Wuhan Customs, Wuhan, Hubei, 430050, China.
[*]E-mail: 153768220@qq.com.

Received: 2 March 2021 / *Accepted:* 14 April 2021 / *Published:* 10 August 2021

A highly sensitive electrochemical nanostructure sensor based on a ZnO@ZIF-8 nanocomposite-modified carbon paste (ZnO@ZIF-8/CPE) electrode was constructed for trace analysis of sulfamethoxazole (SMX). ZnO@ZIF-8 was synthesized by the hydrothermal method and characterized using scanning electron microscopy and X-ray diffraction. Electrochemical experiments demonstrated a synergistic effect of ZnO and ZIF-8 that endowed the prepared sensor with excellent electrocatalytic behavior towards SMX oxidation. Under optimal conditions, the ZnO@ZIF-8/CPE sensor demonstrated a wide linear range of 0.04-50 μM for SMX and a regression coefficient of 0.9914 and a limit of detection of 0.02 μM. The sensor possessed good stability, selectivity, anti-jamming ability and reproducibility and was successfully used for SMX determinations in egg samples. The proposed sensor is ready to use for biomedicine and environmental protection monitoring.

Keywords: carbon paste electrode; ZnO@ZIF-8 nanocomposite; sulfamethoxazole; electrochemical sensor

1. INTRODUCTION

Antibiotics are antimicrobial compounds used in the treatment and prevention of bacterial infections in humans and animals. In particular, antibiotics such as the sulfa drugs are added to animal feeds and act as growth promoters. However, antibiotics are not completely degraded after animal passage and are excreted in urine and feces at high levels. Because of this, maximum residue limits (MRLs) have been proposed [1, 2]. Sulfamethoxazole (SMX) also known as neonomine is a sulfonamide and a broad-spectrum antibiotic that is particularly effective against *Staphylococcus* and *Escherichia coli*. SMX is used in both human and veterinary clinics and is added to animal feeds. The side effects of this drug include skin reactions, blood and liver toxicity [3]. Bacterial drug resistance and the migration

of antibiotic resistance genes (ARG) caused by exposure and accumulation of SMX in the environment are currently pressing problems for human and animal health[4].

The analytical detection of sulfonamides in food and environmental samples has relied on high performance liquid chromatography [5], high performance liquid chromatography-mass spectrometry [6], enzyme-linked immunoassays [7] and capillary electrophoresis [8]. These methods have high sensitivity but also have some shortcomings such as the need for expensive equipment, complex sample pretreatment procedures and long analysis cycles that make them not suitable for on-site analysis or rapid detection. A rapid, simple, sensitive and selective method to monitor SMX and human and animal exposure is therefore necessary for food production, packaging and distribution facilitates.

Electrochemical sensors are a powerful analysis technology that is easy to use, rapid, economical, sensitive and environmentally friendly [9]. Functional support matrices include carbon nanomaterials [10], molecularly imprinted polymers [11], electrically conductive polymers [12] and metal oxides [13] and all have been used to modify sensors to improve their sensitivity and selectivity. Among nanostructured metal oxides, ZnO nanomaterials have both good chemical stability and electron transfer capability and are widely used for photocatalysis [14], photodetectors [15] and biosensors [16] and are examples of stable oxide semiconductors.

Metal-organic frameworks (MOFs) have also been used for catalysis and biomedicine due to their high specific surface areas and excellent chemical and physical properties [17]. In particular, ZIF-8 is a zeolite imidazole-based framework material with a regular dodecahedral sonarite structure. It has a large specific surface area and good thermal stability and is an ideal material for constructing electrochemical sensors [18, 19]. The integrated materials obtained by combining ZIF-8 with carbon nanomaterials [20], metal nanoparticles [21] and ionic liquids [22] enhance the functionality of this MOF. For example, the ZnO@ZIF-8 core-shell heterostructure has shown good electrochemical responses for photocatalysis [23] and biosensors [24].

In this study, we used ZnO nanorods as templates to nucleate a ZIF-8 surface layer to obtain a ZnO@ZIF-8 nanocomposite. We then used this material to modify carbon paste electrodes (CPE) to obtain ZnO@ZIF-8 modified carbon paste electrode (ZnO@ZIF/CPE) and used it for the electrochemical detection of SMX in egg samples. The composite electrode showed high level performance characteristics including high stability, sensitivity and a low detection limit.

2. EXPERIMENTAL

2.1. Chemicals and regents

All solvents and all reagents used in this study were analytical grade or purer. Sulfamethoxazole (SMX) was purchased from Sigma-Aldrich (St. Louis, MO, USA). Zinc acetate ($ZnAc_2 \cdot 2H_2O$), zinc nitrate hexahydrate ($Zn(NO_3)_2 \cdot 6H_2O$) sodium hydroxide (NaOH), 2-methylimidazole (2HmIM), N,N-dimethylformamide (DMF), polyvinylpyrrolidone (PVP), PSA and C_{18} were purchased from Aladdin Biochemical Technology (Shanghai, China) Graphite powder, potassium ferricyanide ($K_3Fe(CN)_6$), potassium ferrocyanide ($K_4Fe(CN)_6 \cdot 3H_2O$), potassium chloride (KCl), phosphoric acid (H_3PO_4), boric

acid, glacial acetic acid, anhydrous sodium acetate (NaAc), anhydrous magnesium sulfate ($MgSO_4$) were purchased from Sinopharm Chemical Reagent (Shanghai, China). Water was obtained in the laboratory from a Milli-R04 purification system (Millipore, Darmstadt, Germany). Britton-Robison buffer (BR) were prepared at different pH values with 0.2 M NaOH and used for SMX dissolution after sonication for 5 min to generate a 1 mM homogeneous stock solution. The stock solutions were stored at 4℃ away from light.

2.2. Apparatus

Electrochemical measurements were performed using a CHI830d electrochemical workstation (Cambria Scientific, Shanghai, China). The traditional three-electrode system was used for the experiments in this work: a modified carbon paste electrode, an Ag/AgCl/KCl (3 M) electrode and a Pt wire electrode served as working electrode, reference electrode and a counter electrode, respectively. All the electrochemical experiments were conducted at room temperature. The pH values of the solutions were measured with Leici PHS-3C pH meter (Precision and Scientific Instruments, Shanghai, China). The structure and morphology of ZIF-8, ZnO and ZnO@ZIF-8 were characterized by powder XRD (Malvern Panalytical, Cambridge, UK) and using a Zeiss Gemini 300 scanning electron microscope (SEM) (Oberkochen, Germany).

2.3. Preparation of ZnO@ZIF-8 composite material

2.3.1. Synthesis of ZnO nanorods

ZnO nanorods were synthesized as previously reported [25]. In brief, 2.2 g $ZnAc_2 \cdot 2H_2O$ and 4 g NaOH were dissolved in 20 mL distilled water and then added to 20 mL aqueous solution containing 0.1g PVP. The mixed solution was sonicated for a few minutes and then transferred to a polytetrafluoroethylene-lined stainless steel autoclave and heated at 180°C for 13 hours. The obtained product was centrifuged, rinsed repeatedly with distilled water and dried under vacuum at 60°C overnight.

2.3.2. Synthesis of ZnO@ZIF-8

ZIF-8 nanorods were grown on the ZnO nanorod template using the hydrothermal method [26] (Fig. 1). In brief, ZnO nanorods (0.5 mmol) and 2HmIM (4 mmol) were added to 40 mL DMF/H_2O (3: 1, V/V) and sonicated for 5 min. The mitigation solution was transferred to a sealed autoclave as per above and heated continuously at 70°C for 24 h. The white product was naturally cooled to room temperature and collected by centrifugation and then washed with DMF and ethanol several times and dried at 60°C for 8 h.

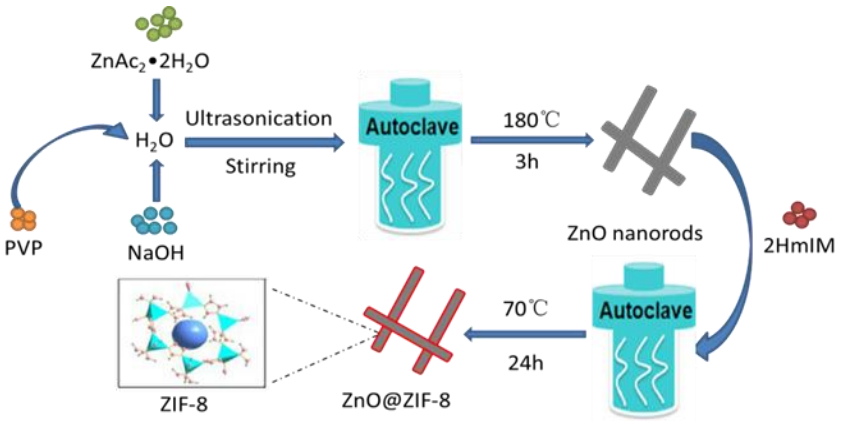

Figure 1. Principle of ZnO@ZIF-8 synthesis

2.4. Preparation of carbon paste electrodes (CPE)

A modified CPE was prepared by mixing ZnO@ZIF-8 with liquid paraffin in a pestle and mortar to form a homogeneous paste. The resulting paste was packed into the well of the PTFE electrode tube to a depth of 2 mm with 3 mm diameter. The paste was fully compacted and polished on weighing paper and dried naturally at room temperature for later use. For control experiments, a bare CPE and ZnO@CPE and ZIF-8@GCE electrodes were prepared using a similar procedure and the corresponding raw materials.

Before use, the blank carbon paste and the modified electrode were scanned using cyclic voltammetry (CV) and a three-electrode system in BR buffer at pH 5. After the CV curve was stabilized, the electrode was removed and rinsed with distilled water and dried for later use.

2.5. Real sample preparation

Real samples were prepared as previously reported with a slight modification [27]. In brief, fresh eggs were purchased from local supermarkets and stored at 4°C until analysis. The whole eggs (yolk and albumen combined) were homogenized at room temperature for 5 min under continuous agitation and 5.0 g of the homogenized sample was placed into 50 mL polypropylene centrifuge tubes. Subsequently, 10 mL of 1 % acetic acid in acetonitrile, 1 g anhydrous NaAc and 3 g anhydrous $MgSO_4$ were added. The mixture was then vortexed for 5 min and centrifuged followed by the addition of 50 mg PSA (ethylenediamino-N-propyl) and 25 mg C_{18}. The mixture was vortexed immediately for another 5 min and centrifuged and then diluted in a volumetric flask using BR buffer for chemical analysis.

3. RESULTS AND DISCUSSION

3.1. Characterization of nanocomposites

The morphologies of ZnO nanorods and ZnO@ZIF-8 nanocomposites were characterized using SEM. The shapes of the ZnO nanorods were cylindroid with smooth surfaces and possessed diameters

of approximately 100 nm with average lengths of 1.5 μm. (Fig. 2A).The majority of ZnO nanorods had assembled into brush-like aggregates that could still be separated with sonication (data not shown). The ZnO@ZIF-8 nanocomposites that formed by the combination of ZIF-8 nanoparticles and ZnO nanorods generated ZIF-8 nanoparticles that had grown scattered on the surface of the nanorods in a polyhedral structure (Fig. 2B).

The XRD patterns of the ZnO nanorods generated sharp and intense diffraction peaks indicative of a high level of crystallinity [28]. The strong diffraction peak of the ZnO@ZIF-8 composite was consistent with the diffraction peak of the pure ZnO nanorod from 30 to 80° indicating that the synthetic material contained ZnO. In conjunction with this, the diffraction peak for ZIF-8[29] that occurred between 10 and 30° indicated that ZIF-8 was successfully recombined onto the ZnO nanorod surface (Fig. 2C). These results indicated that ZnO@ZIF-8 nanocomposites had been successfully synthesized.

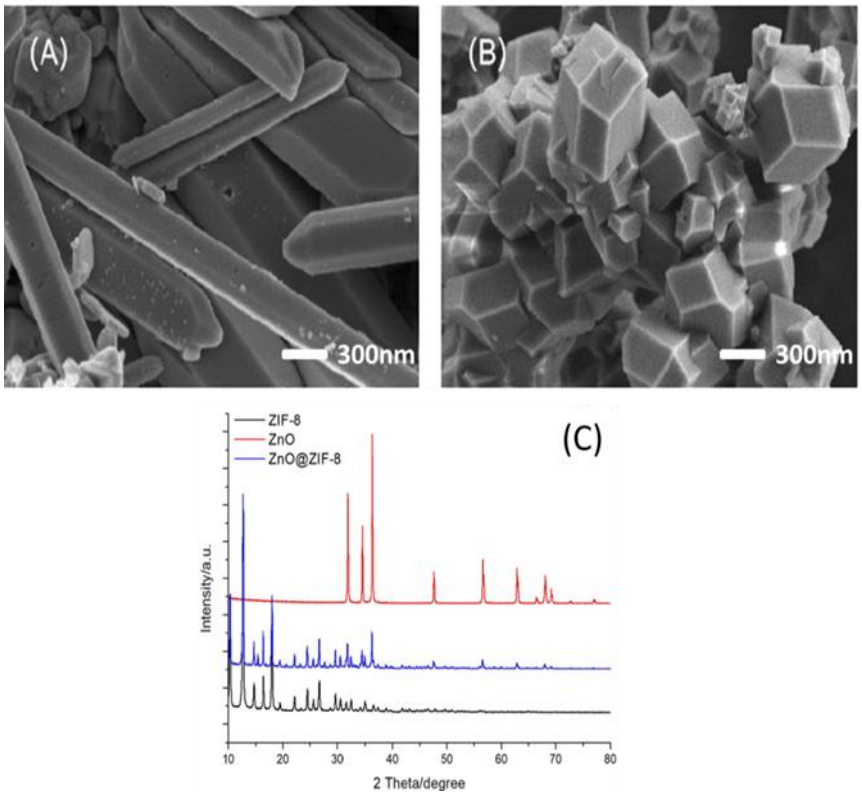

Figure 2. SEM images of (A) ZnO nanorods and (B) ZnO@ZIF-8 nanocomposites. (C) XRD patterns of ZnO nanorods (red), ZIF-8 (black) and ZnO@ZIF-8 nanocomposites (blue)

3.2. Characterization of the modified electrodes

The electrochemical properties of the synthesized electrodes were evaluated using cyclic voltammetry (CV). The four CPEs included the bare electrode (CPE) and the ZnO/CPE, ZIF-8/CPE and ZnO@ZIF-8/CPE sensors were assessed for their abilities to electro-oxidize a 5 mM $K_3Fe(CN)_6$ solution containing 0.1 M KCl at their surfaces. The position of the SMX redox peak in the CV graph is similar to the previous study [30]. All 4 CPEs demonstrated good electrochemical responses to $K_3Fe(CN)_6$ and

a pair of obvious electrochemical redox peaks were apparent. The oxidation peak currents for the bare CPE, ZIF-8/CPE, ZnO/CPE and ZnO@ZIF-8/CPE increased sequentially from 10.77, 14.97, 15.63 and 25.15 μA. The oxidation peak current detected by ZnO@ZIF-8/CPE was 57 % higher than the bare CPE. Additionally, the potential difference was reduced from 168 (bare CPE) to 145 mV (ZnO@ZIF-8-CPE) indicating that ZnO@ZIF-8 increased the electron transfer rate between the $K_3Fe(CN)_6$ solution and the electrode surface and thereby improved the electrocatalytic ability of the electrode (Fig. 3).

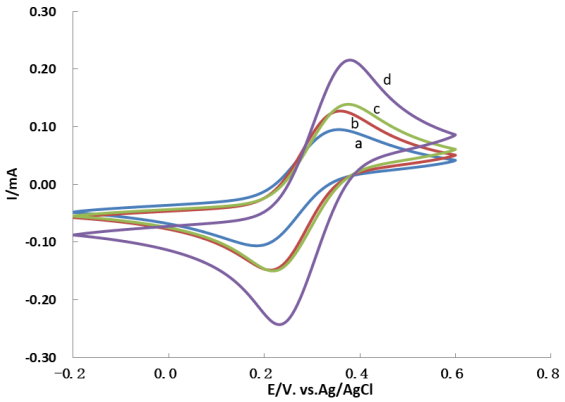

Figure 3. CV curves for the (a) bare CPE (b) ZIF-8/CPE (c) ZnO/CPE and (d) ZnO@ZIF-8/CPE. See text for details Scan rate: 100 mV/s

Electrochemical impedance spectroscopy (EIS) can analyze electrode conductivity during the modification processes [31]. We generated Nyquist plots for the bare CPE, ZIF-8/CPE, ZnO/CPE and ZnO@ZIF-8/CPE in the presence of an external redox probe of 10 mM $[Fe(CN)_6]^{3-/4-}$ (1:1) over a frequency range of 1 to 105 Hz. Generally, Nyquist plots consist of a semicircular portion and a linear portion. The diameter of the semicircle at higher frequencies corresponds to the electron transfer resistance (Ret) while the straight line at lower frequency corresponds to the diffusion process. The Ret value depends on the insulating properties of the dielectric and the electrode-dielectric interface. When the electron transfer rate is high, a smaller semicircle diameter and lower electron transfer resistance would be observed [32].

Compared with the Ret value of the modified electrode in other studies, this study has a smaller Ret value [33]. The maximum Ret value for the bare CPE was 1.15 kΩ and indicative of an inefficient electron transfer process on the CPE surface. In contrast, the Ret of ZIF-8/CPE and ZnO/CPE were 400 and 600 Ω, respectively and indicated that the addition of ZIF-8 and ZnO increased the electron transfer rate. The ZnO@ZIF-8/CPE possessed a Ret of 240 Ω indicating that ZnO@ZIF-8 can accelerate electron transfer and this process plays an important role in promoting electrical conduction (Fig. 4).

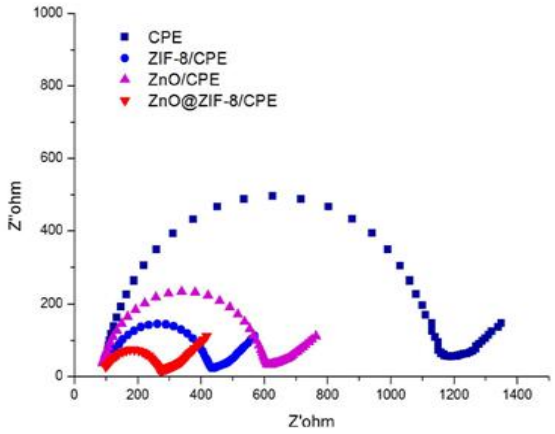

Figure 4. Nyquist plots obtained in 10 mM $[Fe(CN)_6]^{3-/4-}$ (1:1) containing 0.1 M KCl for the 4 electrodes.

3.3. Electrochemical response of SMX

Most of the previous studies used the differential pulse voltammetry (DPV) method to detect SMX [34.35], so we also used differential pulse voltammetry (DPV) responses of the modified electrodes prepared using liquid and solid paraffin in BR buffer solution pH 5.0 that contained 20 µM SMX. In the presence of SMX, a significant oxidation peak was present and increased in the order CPE < ZIF-8/CPE < ZnO/CPE < Zno@zIF-8/CPE. The Zno@ZIF-8 /CPE displayed the best electrochemical performance and were more sensitive to SMX than the other electrodes and generated the highest oxidation peak current (Fig. 5).

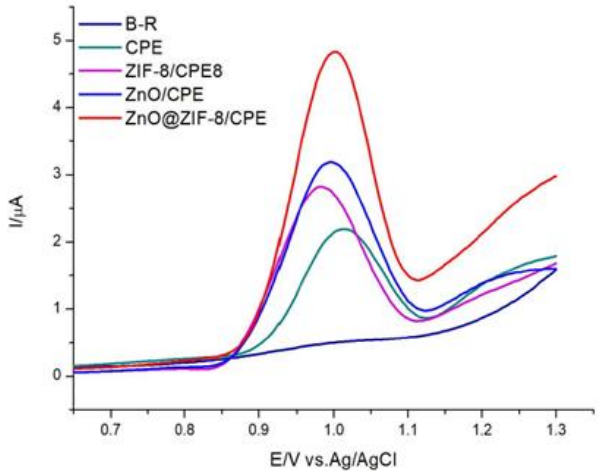

Figure 5. Differential pulse voltammetry scans of the bare CPE, ZIF-8/CPE, ZnO/CPE and ZnO@ZIF-8/CPE in BR buffer pH 5.0 containing 20 µM SMX, Scan rate: 100 mV/s

3.4. Optimization of the method

3.4.1. Optimization of the amount of ZnO@ZIF-8 nanocomposite

The quantity of the ZnO@ZIF-8 nanocomposite used for electrode fabrication has a significant influence on sensor performance [36]. We examined 1, 2.5, 5 and 10 % levels of ZnO@ZIF-8 that were

used to prepare different modified electrodes for SMX detection. When the modification amount was < 5 %, the oxidation peak current of SMX increased in proportion. In contrast, at levels> 5 %, the oxidation peak current decreased accordingly. Therefore, the modification amount of ZnO@ZIF-8 we used for the final sensor was 5 %.

3.4.2. Effects of pH

To investigate the effect of the pH on the electrochemical oxidation of SMX, we conducted DPV tests from pH 3.0 to 8.0 in BR buffer containing 20 μM SMX. We found that the oxidation peaks were pH dependent and the anode peak current of SMX increased as pH increased over the range of 3-8 and reached a maximum at pH 5. At pH > 5, the oxidation peak current for SMX decreased while the peak potential Ep decreased with the increase in pH (Fig. 6A and 6B). This indicated that the electrode reaction was primarily controlled by the proton transfer process [37, 38]. Hence, pH 5.0 was chosen for the remainder of our experiments.

We also determined that there was a linear relationship between Ep and pH and could be expressed by the formula: $E_p(V)=1.2433-0.0478pH$ with an R^2 of 0.9918 (Fig. 6B). The Nernst equation can be used to quantitatively describe the diffusion potential of ions between two systems as follows:

$E_p=E^0+ (0.0591V/n) \log[Ox^a/(Red)^b] - (0.0591V(m/n))pH$

where m and n are the number of protons and electrons transferred in the electrochemical process.

The slope of 0.0512V/pH in our experiments was close to the theoretically expected 0.059V/pH indicating that for the oxidation of SMX on the electrode, the number of electrons and protons involved in the reaction were equal. This slope value was close to that of two electron reactions on the surface of electrodes modified with silver-filled multi-wall carbon nanotubes [39]. Therefore, the number of participating electrons was 2 for this experiment.

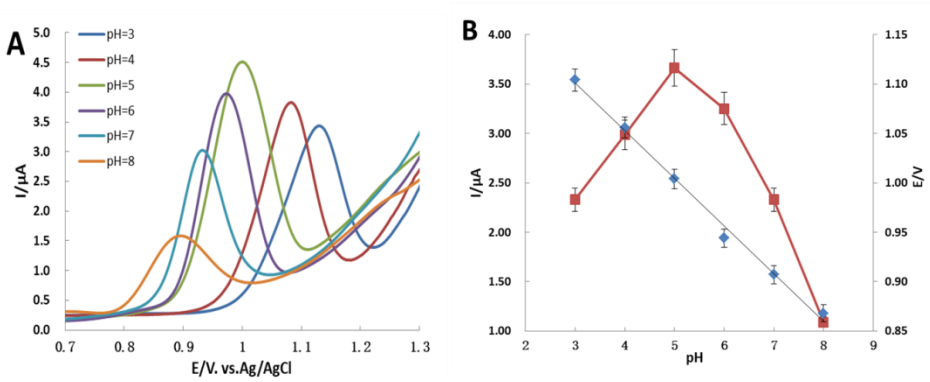

Figure 6. (A) DPV scans for ZnO@ZIF-8-CPE at the indicated pH values; (B) changes of oxidation peak currents at the indicated pH values and the relationship between pH and peak potential (I_P)

3.4.3. Effect of scan rate

The effect of scan rate on the electrochemical reactions of SMX was investigated by CV in BR buffer solution at pH 5 containing 20 μM SMX. When the scan rate was varied from 25 to 200 mV/s,

the oxidation current for SMX increased and shifted slightly positive shift for the oxidation peak potential (Fig. 7A). The scope of the oxidation peak currents for SMX was also linearly related to the square root of the scan rate ($Ip(\mu A) = -0.8509+0.6462\upsilon^{1/2}$, $R^2=0.9997$) indicating that the electrochemical reaction of SMX on ZnO@ZIF-8/CPE was primarily diffusion controlled (Fig. 7B).[40,41]

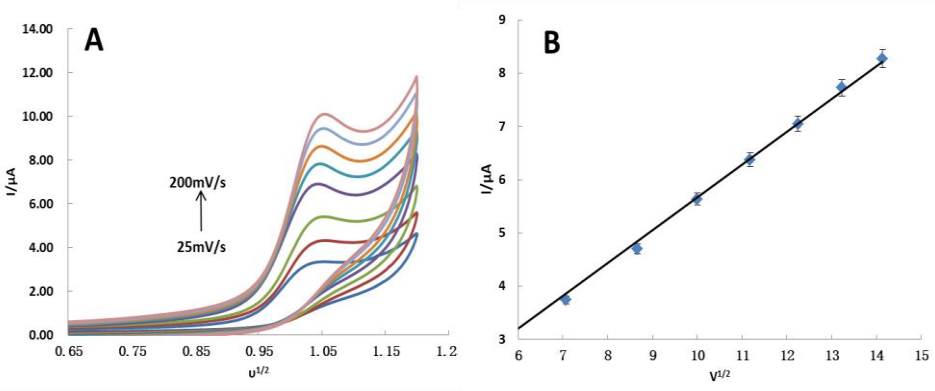

Figure 7. (A) CV response of ZnO@ZIF-8/CPE at the indicated different scanning rates; (B) Linear relationship between $\upsilon^{1/2}$ and I_p

3.5. The electrochemical response of SMX

The DPV method can eliminate the effects that charging current has on background current and was used to detect SMX under optimized experimental conditions using the ZnO@ZIF-8/CPE sensor. As the SMX concentration increased, the peak current intensity also increased (Fig. 8A). We also found a good linear relationship between DPV current and SMX concentration over the range of 0.04 - 50 μM and could be represented by the linear equation: I (μA) = 0.2219 + 0.1533 C (μM), R^2 = 0.9914 (Fig. 8B). This equation was used to calculate the detection limit (LOD) for SMX at 20 nM. This LOD exceeded that reported for other sensors for SMX detection (Table 1) [42].

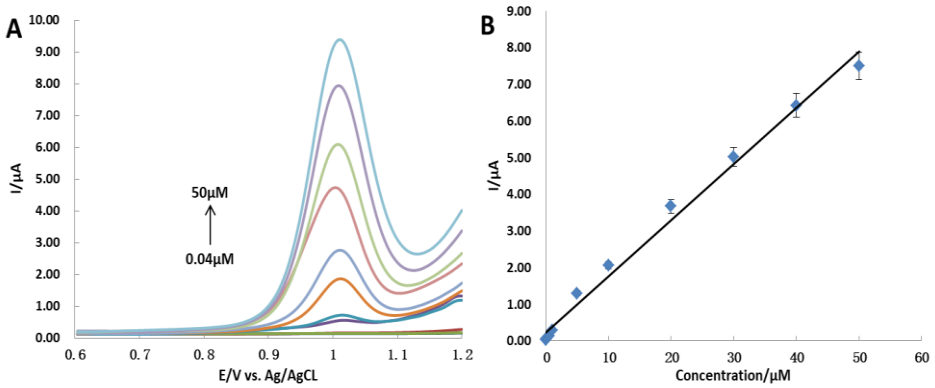

Figure 8. (A) DPV curves for SMX using the ZnO@ZIF-8/CPE sensor (B) Standard curve generated using the values from the DPV voltammogram

Table 1. Comparison of different chemically modified electrodes for SMX determination

Electrode	Detection technique	Linear range (μM)	LOD(μM)	Ref.
Ag-MWCNT/CPE	DPV	0.05-70	0.01	[43]
MWCNT-Nafion/GCE	DPV	50-1000	10	[44]
MIP-OPPy/PGE	DPV	25-750	0.359	[45]
FeZnO/PE	DPV	2-160	0.03	[46]
MIP/GCE	SWV	0.2-1.4	0.05	[47]
MWCNT/ Bnc/SPE	DPV	1-10	0.038	[48]
ZnO@ZIF-8/CPE	DPV	0.04-50	0.03	This work

3.6. Anti-interference ability, reproducibility and stability investigation

The ability of the sensor to detect SMX in the presence of other substances is critical for real world measurements. We examined commons substances that were likely to be present in SMX matrices including glycine, citric acid, urea, ascorbic acid, and sodium chloride at 200-times the concentration of SMX used in the detection system. We used the ZnO@ZIF-8/CPE sensor at an SMZ concentration of 20 μM. The oxidation peak current of the SMX solution in the absence of interfering substances was 3.264 μA. The separate addition of the other test materials listed above generated current signal changes of 2.08, 3.52, 3.08, 2.02 and 2.63 %, respectively. These current signals were within ± 5 % of the pure solution and therefore did not interfere with measurements [49, 50].

The reproducibility of the ZnO@ZIF-8/CPE sensor was studied using DPV in a solution containing 20 μM SMX. Five repeated measurements generated a relative standard deviation (RSD) of 3.0 % and represented a high accuracy level for the sensor. After placing the newly prepared electrode at room temperature for 72 h, the detection signal decreased by about 6.1 % indicating that the electrode has good stability for DPV measurements of SMX.

3.7. Real sample analysis

To evaluate the applicability of ZnO@ZIF-8/CPE to real samples, we used the sensor to determine SMX levels in commercial egg samples.

Table 2. Determination of SMX in homogenized egg samples using the ZnO@ZIF-8/CPE sensor (n=3)

Sample	Added(μM)	Expected(μM)	Founded(μM)	Recovery(%)
Egg	-	-	<LOD	-
	20.0	20.0	19.2±0.91	95.8±2.8

Prior to analysis, the egg samples were pretreated with a QuEChERS method of partial purification [27, 51]. We did not detect SMX in blank egg samples so we used the standard addition method to measure SMX. Our results indicated that the ZnO@ZIF-8/CPE senor can be successfully used for the determination of SMX in real samples (Table 2).

4. CONCLUSIONS

In this study, a ZnO@ZIF-8 composite was synthesized using the hydrothermal method and a ZnO@ZIF-8 modified carbon paste electrode was prepared that was used for the electrochemical determination of SMX. Our results indicated that compared with the bare CPE, the oxidation peak currents for SMX using the ZnO@ZIF-8/CPE sensor were significantly increased as a result of the high specific surface area and rapid electron transfer rates of ZnO@ZIF-8. The sensor possessed high sensitivity with an LOD of 20 nM, excellent selectivity and reliability. Based on the maximum residue limit, the proposed sensor can be used for rapid, simple, efficient and sensitive monitoring of SMX in food matrices.

ACKNOWLEDGEMENTS
This work was supported by the Research Projects of the General Administration of Customs (2019HK091).

References

1. X.Xie, S. Huang, J. Zheng, G. Ouyang, *J Sep. Sci.,* 43(2020) 1634.
2. L. Wang, J. Wu, Q. Wang, C. He, L. Zhou, J. Wang, Q. Pu, *J Agric. Food. Chem.*, 60(2012) 1613.
3. F. Tamtam, F. Mercier, B. Le Bot, J. Eurin, D.Q. Tuc, M. Clement, M. Chevreuil, *Sci. Total Environ.,* 393(2008) 84.
4. C.F. Nnadozie, O.N. Odume, *Environ. Pollut*., 254(2019) 113067.
5. A. Armentano, S. Summa, M.S. Lo, C. Palermo, D. Nardiello, D. Centonze, M. Muscarella, *J. Chromatogr. A*., 1531(2018) 46.
6. E. Dubreil-Cheneau, Y. Pirotais, E. Verdon, D. Hurtaud-Pessel, *J. Chromatogr* A., 1339(2014) 128.
7. Q. Zhou, D. Peng, Y. Wang, Y. Pan, D. Wan, X. Zhang, Z. Yuan, *Food Chem*., 154(2014) 52.
8. T. Dai, J. Duan, X. Li, X. Xu, H. Shi, W. Kang, *Int. J. Mol. Sci*., 18(2017)1286.
9. A. Ait Lahcen, A. Amine, *Anal. Lett*., 51(2018) 424.
10. H. Aleixo, L.L. Okumura, A. Gurgel, A.F.S. Silva, J.A. Diniz, *Anal. Methods*, 11(2019) 1743.
11. A. Turco, S. Corvaglia, E. Mazzotta, *Biosens Bioelectron*., 63(2015) 240.
12. Y.L. Su, S.H. Cheng, *Talanta*, 180(2018) 81.
13. M. Meshki, M. Behpour, S. Masoum, *J. Electroanal. Chem*., 740(2015) 1.
14. K.M. Lee, C.W. Lai, K.S. Ngai, J.C. Juan, *Water Res*., 88(2016) 428.
15. L. Meng, G. Li, X. Tian, S. Bai, Q. Xu, X. Jia, X. Cui, Y. Qin, W. Wu, *ACS Appl. Mater. Interfaces*., 12(2020) 1054.
16. S.K. Arya, S. Saha, J.E. Ramirez-Vick, V. Gupta, S. Bhansali, S.P. Singh, *Anal. Chim. Acta*, 737(2012) 1.
17. J. Yang, Y.W. Yang, *Small*, 16(2020) e1906846.
18. W. Zhang, L. Zong, S. Liu, S. Pei, Y. Zhang, X. Ding, B. Jiang, Y. Zhang, *Biosens. Bioelectron*., 131(2019) 200.

19. J. Yang, H. Ye, F. Zhao, B. Zeng, *ACS Appl. Mater. Interfaces*, 8(2016) 20407.
20. J.A. El, L. Yan, J. Zhu, D. Zhao, H.K.M. Zaved, X. Liu, *Anal. Chim. Acta*, 1106(2020) 103.
21. A. Samadi-Maybodi, S. Ghasemi, H. Ghaffari-Rad, *Sens. Actuators*, B., 220(2015) 627.
22. L. Wei, X. Huang, L. Zheng, J. Wang, Y. Ya, F. Yan, *Ionics*, 25(2019) 5013-5021.
23. X. Wang, J. Liu, S. Leong, X. Lin, J. Wei, B. Kong, Y. Xu, Z.X. Low, J. Yao, H. Wang, *ACS Appl. Mater. Interfaces*, 8(2016) 9080.
24. S. Dong, M. Tong, D. Zhang, T. Huang, *Sens. Actuators*, B., 251(2017) 650.
25. X. Duan, G. Chen, C. Li, Y. Yin, W. Jin, L. Guo, H. Ye, Y. Zhu, Y. Wu, *Nanotechnology*, 27(2016) 295601.
26. H. Tian, H. Fan, M. Li, L. Ma, *ACS Sens*., 1(2016) 243.
27. X. Xu, X. Xu, M. Han, S. Qiu, X. Hou, *Food. Chem*., 276(2019) 419.
28. X. Yue, Z. Li, S. Zhao, *Microchem. J*., 159(2020) 105440.
29. Y. Feng, L. Zhong, M. Bilal, Z. Tan, Y. Hou, S. Jia, J. Cui, *Polymers (Basel).,* 11(2018).
30. A. Turco, S. Corvaglia, E. Mazzotta, P.P. Pompa, C. Malitesta, *Sens. Actuators* B., 255(2018) 3374.
31. X. Yue, Z. Li, S. Zhao, *Microchem. J*., 159(2020)105440.
32. B.Y. Chang, S.M. Park, *Annu. Rev. Anal. Chem (Palo Alto Calif).,* 3(2010) 207.
33. L.F. Sgobbi, C.A. Razzino, S.A.S. Machado, *Electrochim. Acta*, 191(2016) 1010-1017.
34. A. Yari, A. Shams, *Anal. Chim. Acta*, 1039(2018) 51.
35. C. Chen, Y. Chen, Y. Hong, T. Lee, J. Huang, *Chem. Eng. J.,* 352(2018) 188-197.
36. X. Huang, C. Duan, W. Duan, F. Sun, H. Cui, S. Zhang, X. Chen, *J. Cleaner Prod., Available online 3 April* 2021, 126951.
37. M.R. Shishehbore, H.R. Zare, D. Nematollahi, M. Saber-Tehrani, *Anal. Methods*, 3(2011) 306.
38. A. Yari, A. Shams, *Anal. Chim. Acta*, 1039(2018) 51.
39. L. Jothi, S. Neogi, S.K. Jaganathan, G. Nageswaran, *Biosens. Bioelectron.,* 105(2018) 236.
40. L. Bard, M. Electrochemical Methods: Fundamentals and Applications, 2000.
41. A. Turcoa, S. Corvaglia, E. Mazzotta, P. Pompa, C. Malitesta, *Sens. Actuators* B., 255 (2018) 3374.
42. A M. Committee, *Analyst (Cambridge, U. K.).,* 112(1987) 199.
43. A. Yari, A. Shams, *Anal. Chim. Acta*, 1039(2018) 51.
44. S. Issac, K.K. Girish, *Drug Test. Anal*., 1(2009) 350.
45. S.P. Ozkorucuklu, Y. Sahin, G. Alsancak, *Sensors (Basel),* 8(2008) 8463-8478.
46. H. Zhang, *Int J. Electrochem. Sc*., (2019) 11630-11640.
47. L.F. Sgobbi, C.A. Razzino, S.A.S. Machado, *Electrochim. Acta*, 191(2016) 1010.
48. M. Shabani-Nooshabadi, M. Roostaee, *J. Mol. Liq*., 220(2016) 329-333.
49. A. Arroquia, I. Acosta, M. Armada, *Mater. Sci. Eng. C Mater. Biol. Appl*., 109(2020) 110602.
50. D. Chen, X. Sun, Y. Guo, L. Qiao, X. Wang, *Bioprocess Biosyst Eng*, 38(2015) 315-321.
51. J.F. Huertas-Perez, N. Arroyo-Manzanares, L. Havlikova, L. Gamiz-Gracia, P. Solich, A.M. Garcia-Campana, *J. Pharm. Biomed. Anal.,* 124(2016) 261-266